Supplementary Text for: "Maturation models of fluorescent proteins are necessary for unbiased estimates of promoter activity"

Antrea Pavlou[1,2], Eugenio Cinquemani[1], Johannes Geiselmann[2*+], and Hidde de Jong[1*+]

[1]Univ. Grenoble Alpes, Inria, Grenoble, France.
[2]Univ. Grenoble Alpes, CNRS, LIPhy, Grenoble, France
[*]these authors contributed equally to this work
[+]corresponding authors

S1 Model definition, calibration and selection

S1.1 Model equations

The models are defined on the population-level: they describe the total quantity of protein species (red, green, blue, colorless) in a growing population of cells. Protein quantities are expressed in relative fluorescence units (RFU), assumed proportional to molar units. We disntinguish between $\mathrm{RFU}_{\mathrm{green}}$, $\mathrm{RFU}_{\mathrm{red}}$, and $\mathrm{RFU}_{\mathrm{blue}}$ to quantify green, red, and blue fluorescence, respectively. Biomass is quantified by absorbance (Abs), assumed proportional to the volume of bacterial population.

GFP model:

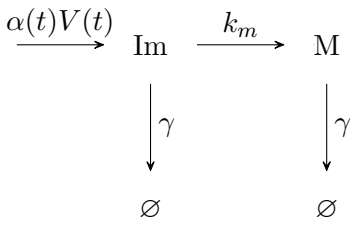

$$\frac{d}{dt}Im(t) = \alpha(t) \cdot V(t) - (\gamma + k_m) \cdot Im(t), \tag{S1}$$

$$\frac{d}{dt}M(t) = k_m \cdot Im(t) - \gamma \cdot M(t). \tag{S2}$$

For GFP, we assume that immature protein is produced at a rate $\alpha(t) \cdot V(t)$, where $\alpha(t)$ [$\mathrm{RFU}_{\mathrm{green}}$ min^{-1} Abs^{-1}] is the specific production rate, per unit population volume, and $V(t)$ [Abs] the

volume of the growing population. The specific production rate is also called promoter activity in the literature, assuming that the dynamics of the intermediate mRNA species can be ignored [1]. The quantity of immature proteins $Im(t)$ is expressed in the same units as the quantity of mature proteins $M(t)$, $\mathrm{RFU}_{\mathrm{green}}$, which allows for their direct comparison. The conversion of immature to mature protein occurs at a rate proportional to the quantity of immature protein with constant k_m [min^{-1}] and all proteins are degraded at the same rate with rate constant γ [min^{-1}] (see Table S1.1 for parameters and units).

RFP models:
The RFP model is composed of three variables, modeling the quantity of immature protein $Im(t)$, intermediate blue protein $Hm(t)$, and mature red protein $M(t)$, with appropriate rate constants for inter-species conversion $k_{hm}^{+}, k_{hm}^{-}, k_{m}^{+}, k_{m}^{-}$. All protein quantities are expressed in red fluorescence units $\mathrm{RFU}_{\mathrm{red}}$. In the next section, we introduce a conversion of red fluorescence units to blue fluorescence units, in order to allow $Hm(t)$ to be related to measurements of this blue intermediate.

We consider four variants of the RFP model (I-IV) having zero, one or two backflows, since we have no prior information on the reversibility of each reaction.

I

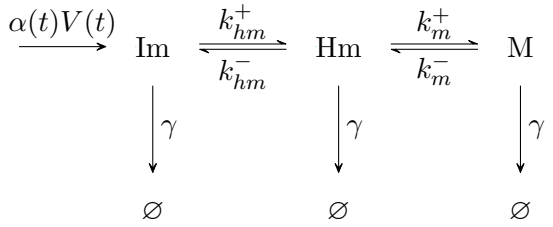

$$\frac{d}{dt}Im(t) = \alpha(t) \cdot V(t) - (k_{hm}^{+} + \gamma) \cdot Im(t) + k_{hm}^{-} \cdot Hm(t), \tag{S3}$$

$$\frac{d}{dt}Hm(t) = k_{hm}^{+} \cdot Im(t) - (k_{hm}^{-} + k_{m}^{+} + \gamma) \cdot Hm(t) + k_{m}^{-} \cdot M(t), \tag{S4}$$

$$\frac{d}{dt}M(t) = k_{m}^{+} \cdot Hm(t) - (k_{m}^{-} + \gamma) \cdot M(t). \tag{S5}$$

II

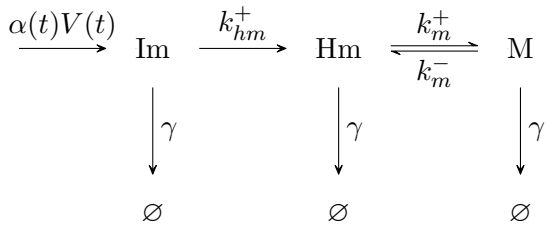

$$\frac{d}{dt}Im(t) = \alpha(t) \cdot V(t) - (k_{hm}^{+} + \gamma) \cdot Im(t), \tag{S6}$$

$$\frac{d}{dt}Hm(t) = k_{hm}^{+} \cdot Im(t) - (k_{m}^{+} + \gamma) \cdot Hm(t) + k_{m}^{-} \cdot M(t), \tag{S7}$$

$$\frac{d}{dt}M(t) = k_{m}^{+} \cdot Hm(t) - (k_{m}^{-} + \gamma) \cdot M(t). \tag{S8}$$

III

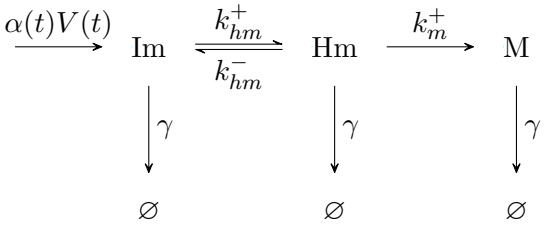

$$\frac{d}{dt}Im(t) = \alpha(t) \cdot V(t) - (k_{hm}^{+} + \gamma) \cdot Im(t) + k_{hm}^{-} \cdot Hm(t), \tag{S9}$$

$$\frac{d}{dt}Hm(t) = k_{hm}^{+} \cdot Im(t) - (k_{hm}^{-} + k_{m}^{+} + \gamma) \cdot Hm(t), \tag{S10}$$

$$\frac{d}{dt}M(t) = k_{m}^{+} \cdot Hm(t) - \gamma \cdot M(t). \tag{S11}$$

IV

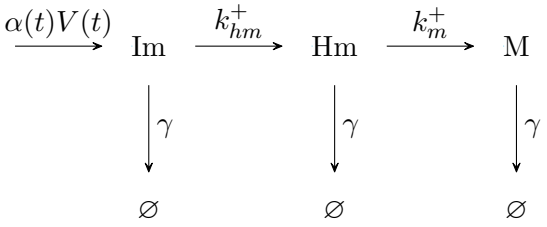

$$\frac{d}{dt}Im(t) = \alpha(t) \cdot V(t) - (k_{hm}^{+} + \gamma) \cdot Im(t), \tag{S12}$$

$$\frac{d}{dt}Hm(t) = k_{hm}^{+} \cdot Im(t) - (k_{m}^{+} + \gamma) \cdot Hm(t), \tag{S13}$$

$$\frac{d}{dt}M(t) = k_{m}^{+} \cdot Hm(t) - \gamma \cdot M(t). \tag{S14}$$

Parameter	Definition	Meaning	Units
k_{hm}^{+}	$\in \mathbb{R}_{+}$	maturation constant	min^{-1}
k_{hm}^{-}	$\in \mathbb{R}_{+}$	maturation constant	min^{-1}
k_{m}^{+}	$\in \mathbb{R}_{+}$	maturation constant	min^{-1}
k_{m}^{-}	$\in \mathbb{R}_{+}$	maturation constant	min^{-1}
k_{hm}	$\in \mathbb{R}_{+}$	maturation constant	min^{-1}
k_{m}	$\in \mathbb{R}_{+}$	maturation constant	min^{-1}
γ	$\in \mathbb{R}_{+}$	degradation constant	min^{-1}
$\alpha(t)$	$\in \mathbb{R}_{+}$	promoter activity	$\text{RFU}_{\text{green/red}}\ \text{min}^{-1}\ \text{Abs}^{-1}$
$V(t)$	$\in \mathbb{R}_{+}$	population volume	Abs
z	$\in \mathbb{R}_{+}$	fluorescence correction factor	$\text{RFU}_{\text{red}}/\text{RFU}_{\text{blue}}$
$Im(t)$, $M(t)$	$\in \mathbb{R}_{+}$	quantity of (im)mature protein	$\text{RFU}_{\text{green/red}}$
$Hm(t)$	$\in \mathbb{R}_{+}$	quantity of half-mature protein	RFU_{red}
$\overline{Hm}(t)$	$\in \mathbb{R}_{+}$	quantity of half-mature protein	RFU_{blue}

Table S1.1: Definition and units of variables and parameters in the maturation models for GFP and RFP.

S1.2 Equations used for model calibration

For the calibration of the models and model selection, we performed experiments where we added Chloramphenicol (Cm), a translation inhibitor, to growing cultures of bacteria containing the two reporter proteins (*Materials and methods*). When Cm is added, no new proteins are synthesized and biomass does not further accumulate (Fig. S1). Therefore, $\alpha = 0$ in the models and all increase in fluorescence can only result from maturation of residual immature protein. The observed fluorescence curves display dynamics on two different time-scales (Fig. S1). In the initial phase, in the first tens of minutes after Cm addition, maturation is dominating the dynamics and the effect of degradation can be neglected. The fluorescent proteins are stable with half-lives on the order of 10-20 h, so that $\gamma \ll k_{m}^{+}, k_{hm}^{+}, \ldots$. After this initial phase, almost all proteins are mature ($Im(t) = Hm(t) \approx 0$) and degradation is dominating, on a time-scale of (tens of) hours.

S1.2.1 Identification of maturation parameters

In the absence of protein synthesis and negligible effect of degradation, we can write the conservation relation in the case of RFP models:

$$m_t = Im(t) + Hm(t) + M(t), \tag{S15}$$

where m_t is the constant total amount of proteins. Fro Eq. S15 it follows that $Im(t) = m_t - Hm(t) - M(t)$. $Im(t)$ equals $Im_0 + Hm_0 + M_0 - Hm(t) - M(t)$, where the index $_0$ refers to the initial protein quantity at the time of Cm addition, given that $m_t = Im_0 + Hm_0 + M_0$. We can eliminate variable Im and the corresponding equation for each model variant to obtain a system with two equations. In the case of variant I this gives:

$$\frac{d}{dt}Hm(t) = k_{hm}^{+} \cdot (Im_0 + Hm_0 + M_0 - Hm(t) - M(t)) - (k_{hm}^{-} + k_m^{+}) \cdot Hm(t) + k_m^{-} \cdot M(t), \quad \text{(S16)}$$

$$\frac{d}{dt}M(t) = k_m^{+} \cdot Hm(t) - k_m^{-} \cdot M(t). \quad \text{(S17)}$$

As explained above, the fluorescent proteins are all expressed in units $\mathrm{RFU_{red}}$, in order to make their quantities comparable. This requires a constant rescaling factor z [$\mathrm{RFU_{red}\ RFU_{blue}}^{-1}$] to relate the variable Hm to the blue fluorescence emitted by the half-mature proteins:

$$Hm = z \cdot \overline{Hm}, \quad \text{(S18)}$$

where $\overline{Hm}$ represents the quantity of half-mature proteins in units $\mathrm{RFU_{blue}}$.

Thus, the ODE system becomes:

$$z \cdot \frac{d}{dt}\overline{Hm}(t) = k_{hm}^{+} \cdot (Im_0 + z \cdot \overline{Hm}_0 + M_0 - z \cdot \overline{Hm}(t) - M(t)) - z \cdot (k_{hm}^{-} + k_m^{+}) \cdot \overline{Hm}(t) + k_m^{-} \cdot M(t), \quad \text{(S19)}$$

$$\frac{d}{dt}M(t) = k_m^{+} \cdot z \cdot \overline{Hm}(t) - k_m^{-} \cdot M(t). \quad \text{(S20)}$$

With the same reasoning, we obtain for model II:

$$z \cdot \frac{d}{dt}\overline{Hm}(t) = k_{hm}^{+} \cdot (Im_0 + z \cdot \overline{Hm}_0 + M_0 - z \cdot \overline{Hm}(t) - M(t)) - (k_m^{+} + k_{hm}^{-}) \cdot z \cdot \overline{Hm}(t), \quad \text{(S21)}$$

$$\frac{dM(t)}{dt} = k_m^{+} \cdot z \cdot \overline{Hm}(t), \quad \text{(S22)}$$

for model III:

$$z \cdot \frac{d}{dt}\overline{Hm}(t) = k_{hm}^{+} \cdot (Im_0 + z \cdot \overline{Hm}_0 + M_0 - z \cdot \overline{Hm}(t) - M(t)) - k_m^{+} \cdot z \cdot \overline{Hm}(t) + k_m^{-} \cdot M(t), \quad \text{(S23)}$$

$$\frac{d}{dt}M(t) = k_m^{+} \cdot z \cdot \overline{Hm}(t) - k_m^{-} \cdot M(t), \quad \text{(S24)}$$

and for model IV:

$$z \cdot \frac{d}{dt}\overline{Hm}(t) = k_{hm}^{+} \cdot (Im_0 + z \cdot \overline{Hm}_0 + M_0 - z \cdot \overline{Hm}(t) - M(t)) - k_m^{+} \cdot z \cdot \overline{Hm}(t), \quad \text{(S25)}$$

$$\frac{d}{dt}M(t) = k_m^{+} \cdot z \cdot \overline{Hm}(t). \quad \text{(S26)}$$

In the case of GFP, we have a single model without backflow. With the same simplifications as for RFP, we obtain the following equation for the estimation of k_m from the fluorescence data:

$$\frac{d}{dt}M(t) = k_m \cdot (Im_0 + M_0 - M(t)). \quad \text{(S27)}$$

S1.2.2 Identification of degradation parameter

For the estimation of the degradation constant γ, we only considered the RFP model without backflows (IV), since this model variant was retained for the analysis (see below). This yields the following model to be fitted against the fluorescence data:

$$\frac{d}{dt}M(t) = -\gamma \cdot M(t)). \tag{S28}$$

The same model was used for GFP.

S1.3 Parameter estimation and model selection

The models defined above were calibrated by means of the experimental data in Fig. 3C-D and Fig. S1. Each model was fitted to the corresponding red/blue or green fluorescence data and the R^2 for each measured protein species was calculated. Parameters k^+_{hm}, k^-_{hm}, k^+_m, k^-_m along with the initial quantity of Im (Im_0) and the RFU conversion factor z were estimated from the data from the first tens of minutes of the calibration experiment (Fig. 3C-D). The parameter γ was estimated from the final four to eight hours of the experiment (Fig. S1). The method of least-squares via the Python function `lmfit.minimize` was used to produce the best fit. For the calibration of the RFP models, the residuals produced from the blue fluorescence curve were multiplied with the conversion factor z so that blue and red residuals are in the same scale. The estimated parameters for each models are presented in Table S1.2.

In parallel, for each RFP model variant the Akaike Information Criterion (AIC) was calculated [2]. We selected the model with the lowest AIC which is model IV, the model without backflows. For the selected model the superscript + is dropped in the main text for convenience (*i.e.*, $k_m = k^+_m$ and $k_{hm} = k^+_{hm}$). We also fitted a one-step model to the red fluorescence data, in order to assess any differences with the two-step model in the analysis of the data from the validation experiment (Fig. S11).

Model	k^+_{hm}	k^-_{hm}	k^+_m	k^-_m	γ	z	Im_0	R^2_m	R^2_{hm}	AIC
RFP I	4e-7	0.006	0.105	8e-10	0.0001	1.01	7043	0.999	0.913	3528
RFP II	0.020	0.104	0.104	-	0.0001	1.01	24480	0.999	0.913	3625
RFP III	0.020	-	0.104	7e-12	0.0001	1.01	24480	0.999	0.913	3625
RFP IV	0.020	-	0.105	-	0.0001	1.01	24476	0.999	0.913	3524
GFP	-	-	0.080	-	0.0002	-	5222	0.972	-	-
RFP one-step	-	-	0.019	-	0.0001	-	7680	0.997	-	-

Table S1.2: Parameter estimates for each model. The method of least-squares was used by minimising the sum of squares of the residuals to obtain the best fit.

An *a-posteriori* bootstrapping procedure was also performed to check for identifiability issues in the RFP model variants [3]. 1000 new datasets were created by randomly assigning the residuals obtained from the best fit to the data of Fig. 1C. The resulting datasets were used to fit each one of the four RFP maturation models. Fig. S14 demonstrates the parameter values estimated from the bootstrap datasets relative to the estimated values from the actual dataset (Table

S1.2). The identifiability analysis shows that the parameters for the selected model variant (IV) can be determined with high precision from the data, contrary to the other model variants (Fig. S14).

References

[1] de Jong, H., C. Ranquet, D. Ropers, C. Pinel, and J. Geiselmann, 2010. Experimental and computational validation of models of fluorescent and luminescent reporter genes in bacteria. *BMC Syst Biol* 4:55.

[2] Sakamoto, Y., M. Ishiguro, and G. Kitagawa, 1986. Akaike Information Criterion Statistics. Springer Netherlands, Dordrecht.

[3] Stefan, D., C. Pinel, S. Pinhal, E. Cinquemani, J. Geiselmann, and H. de Jong, 2015. Inference of quantitative models of bacterial promoters from time-series reporter gene data. *PLoS Comput Biol* 11:e1004028.

Supplementary Figures for: "Maturation models of fluorescent proteins are necessary for unbiased estimates of promoter activity"

Antrea Pavlou[1,2], Eugenio Cinquemani[1], Johannes Geiselmann[2*+], and Hidde de Jong[1*+]

[1]Univ. Grenoble Alpes, Inria, Grenoble, France.
[2]Univ. Grenoble Alpes, CNRS, LIPhy, Grenoble, France
[*]these authors contributed equally to this work
[+]corresponding authors

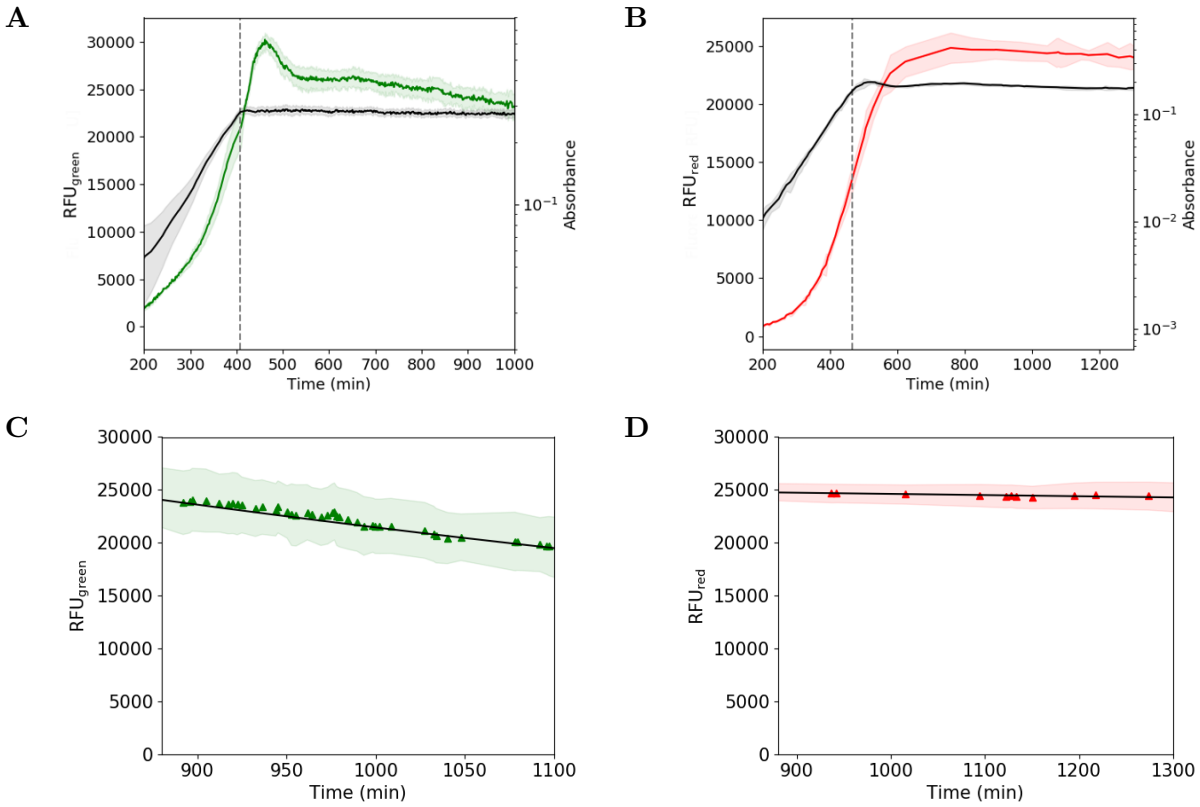

Figure S1: Absorbance and fluorescence levels in calibration experiments. The reporter strains expressing GFPmut2 or mScarlet-I were grown in MOPS medium supplemented with glucose. Chloramphenicol (Cm) was added to the medium to stop translation (dashed gray lines). (**A**) Measurement of absorbance (black curve) and green fluorescence (green triangles) for the GFP strain. (**B**) Measurement of absorbance (black curve) and red fluorescence (red triangles) for the RFP strain. The plots show the mean of 6 replicates and a confidence interval given by twice the standard error of the mean. After addition of Cm, the biomass stops accumulating after a short initial delay. The fluorescence intensity initially increases, due to maturation of the newly synthesized proteins before translation arrest. Eventually, the intensity decreases due to degradation of the fluorescent proteins. These two stages of the fluorescence dynamics are used for the calibration of the model. (**C**) Fit of maturation model to the GFP data when estimating the degradation constant γ (Text S1). (**D**) Idem for the RFP data.

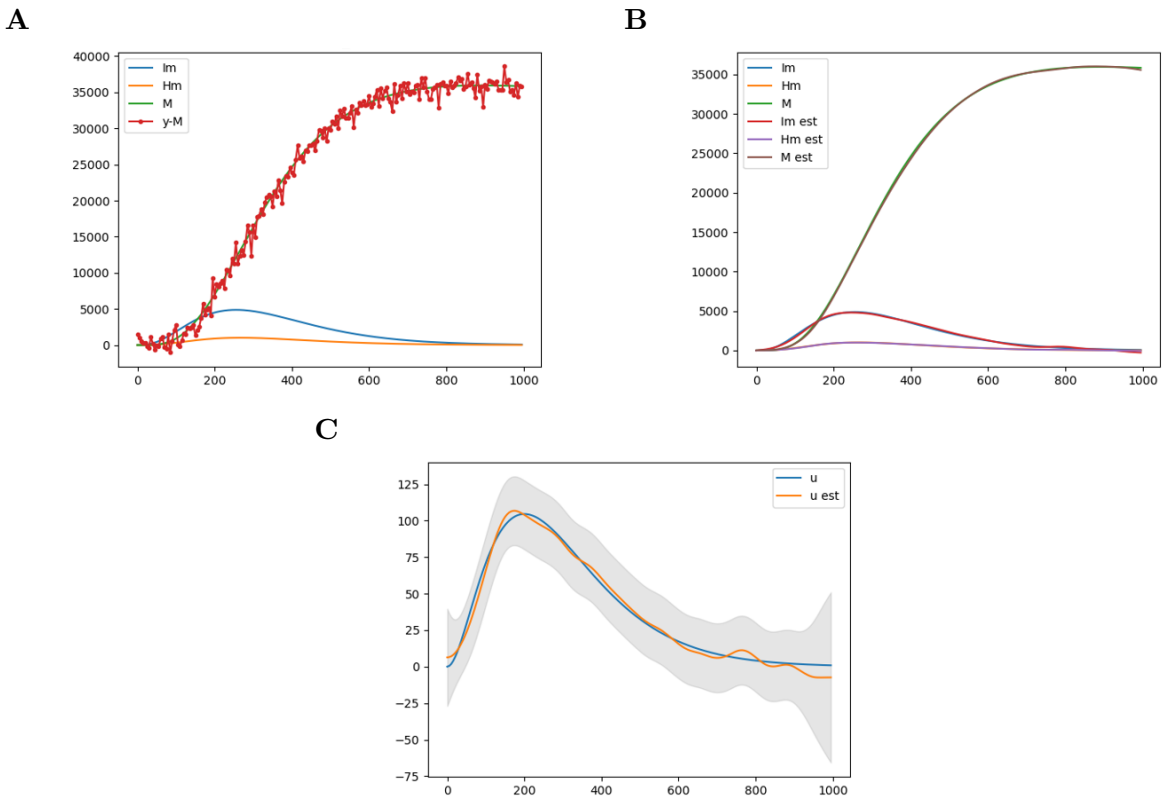

Figure S2: Performance of the Bayesian inference approach on synthetic data. (**A**) Synthetic data generated from a fixed promoter activity profile, using the model of Eqs 3-5 with added random white noise $\sim N(0, 1000)$ (red curve). (**B**) Estimated quantities for each species (Im est, Hm est, M est) *vs* generated quantities (Im, Hm, M). The estimation procedure uses the Kalman filtering/smoothing approach described in the *Materials and methods*. As can be seen, the generated and estimated quantities almost perfectly coincide. (**C**) Reconstructed promoter activity profile and confidence interval compared to the promoter activity used to generate the data (u est and u, respectively). The algorithm is capable of robustly reconstructing the promoter activity profiles from synthetic data.

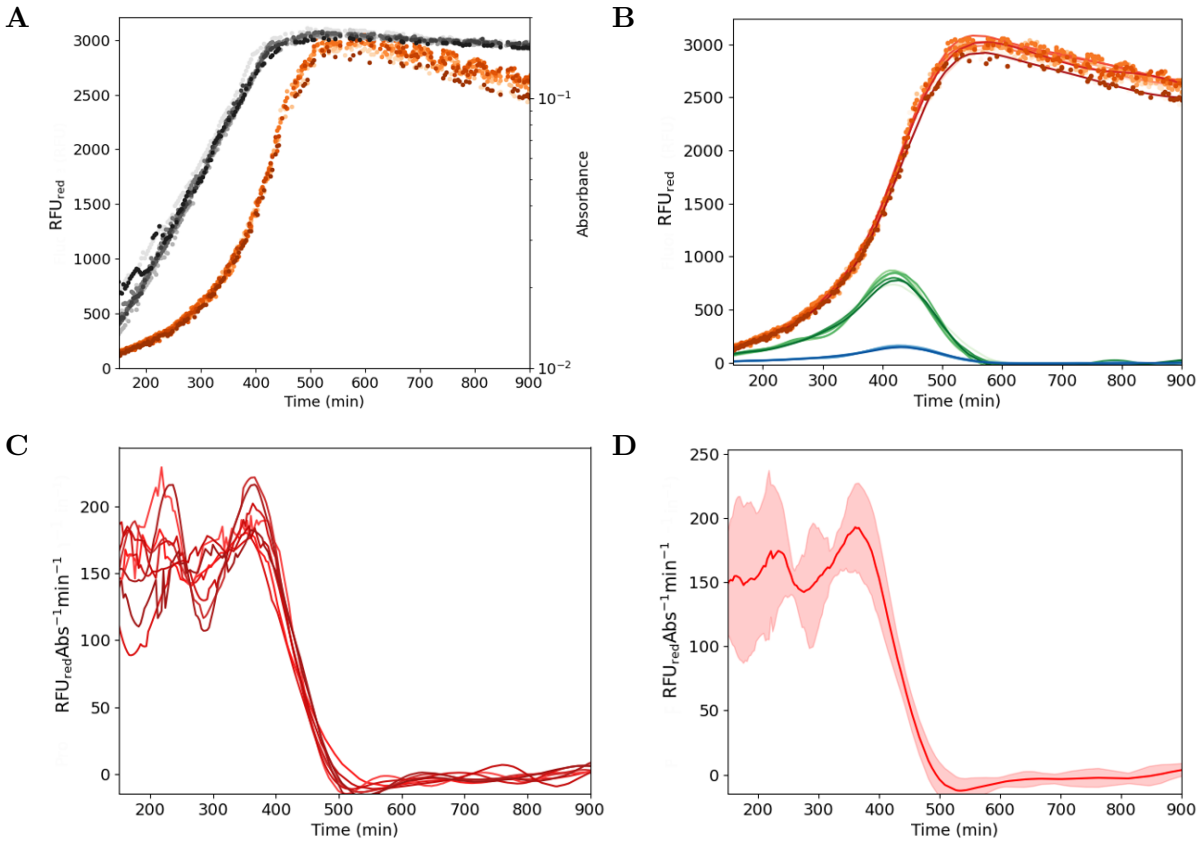

Figure S3: Reconstruction of promoter activities from RFP data of bacteria growing in minimal medium with glucose. (**A**) Red fluorescence (orange to red dots) and absorbance (grey to black dots) for 8 replicates. (**B**) Estimation of $Im(t)$ (green curves), $Hm(t)$ (blue curves) and $M(t)$ (orange to red curves) using the RFP maturation model and the data from panel A, also presented here (orange to red dots). (**C**) Reconstruction of individual promoter activities for each replicate using the Bayesian inference procedure. (**D**) Mean of reconstructed promoter activities and confidence intervals given by two times the standard error of the mean. The curve in panel D corresponds to the promoter activity profile shown in Fig. 3D in the main text.

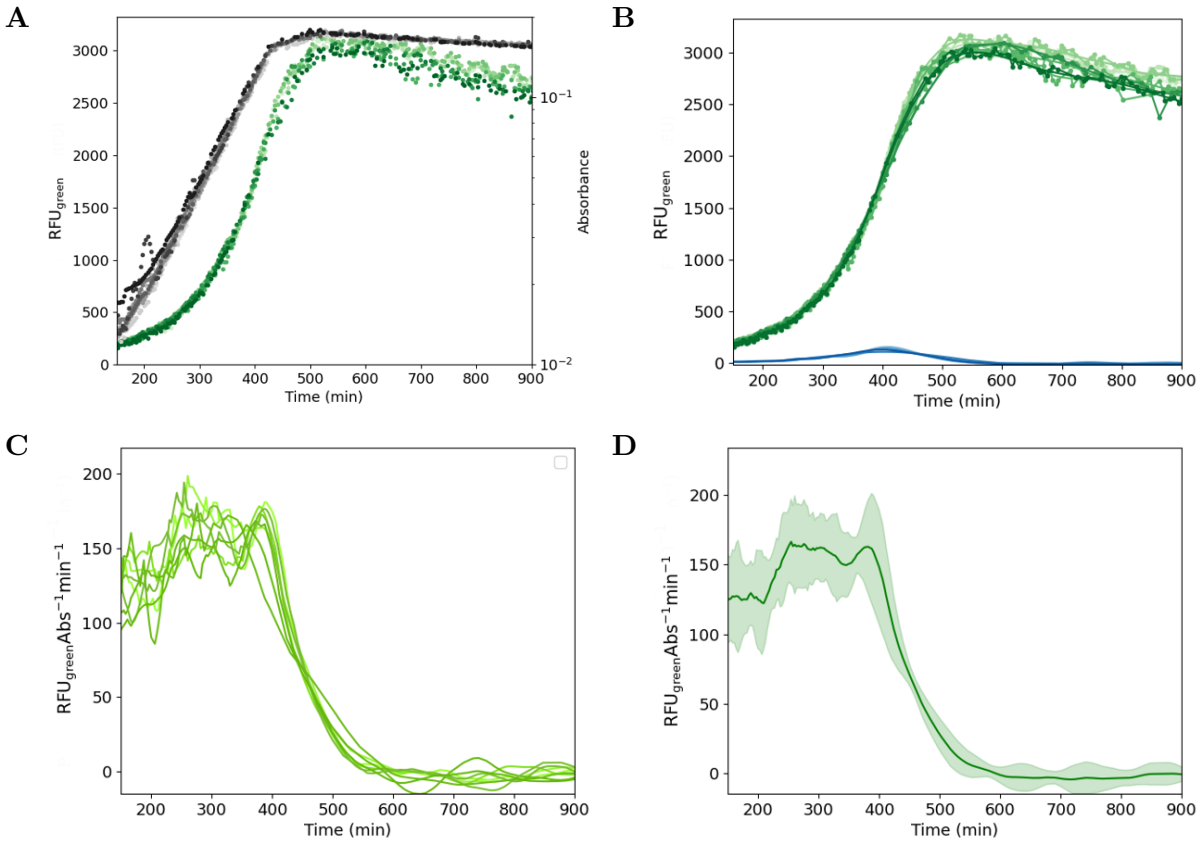

Figure S4: Reconstruction of promoter activities from GFP data of bacteria growing in minimal medium with glucose. (**A**) Green fluorescence (green dots) and absorbance (grey to black dots) for 8 replicates. (**B**) Estimation of $Im(t)$ (blue curves) and $M(t)$ (green curves) using the GFP maturation model and the data from panel A, also presented here (green dots). (**C**) Reconstruction of individual promoter activities for each replicate using the Bayesian inference procedure. (**D**) Mean of reconstructed promoter activities and confidence intervals given by two times the standard error of the mean. The curve in panel D corresponds to the promoter activity profile shown in Fig. 3D in the main text.

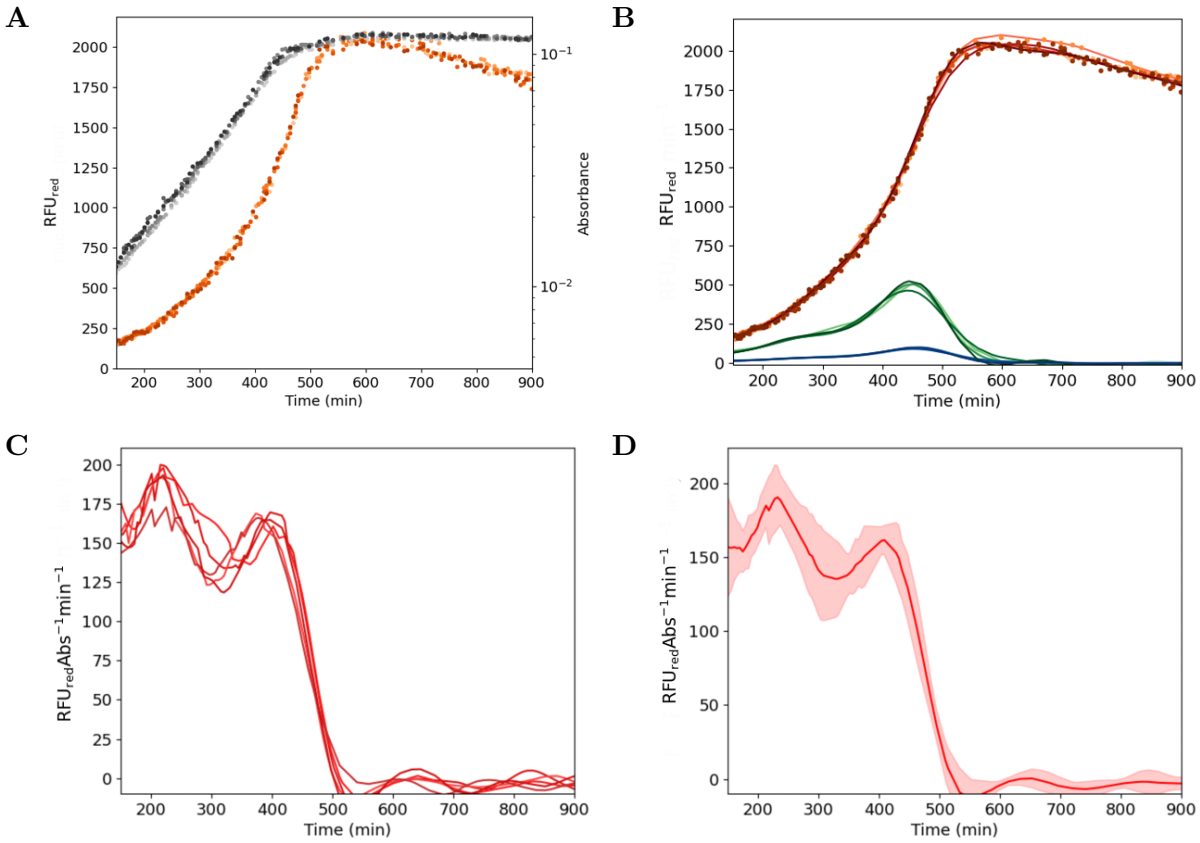

Figure S5: Reconstruction of promoter activities from RFP data of bacteria growing in minimal medium with xylose. (**A**) Red fluorescence (orange to red dots) and absorbance (grey to black dots) for 4 replicates. (**B**) Estimation of $Im(t)$ (green curves), $Hm(t)$ (blue curves) and $M(t)$ (orange to red curves) using the RFP maturation model and the data from panel A, also presented here (orange to red dots). (**C**) Reconstruction of individual promoter activities for each replicate using the Bayesian inference procedure. (**D**) Mean of reconstructed promoter activities and confidence intervals given by two times the standard error of the mean. The curve in panel D corresponds to the promoter activity profile shown in Fig. 3E in the main text.

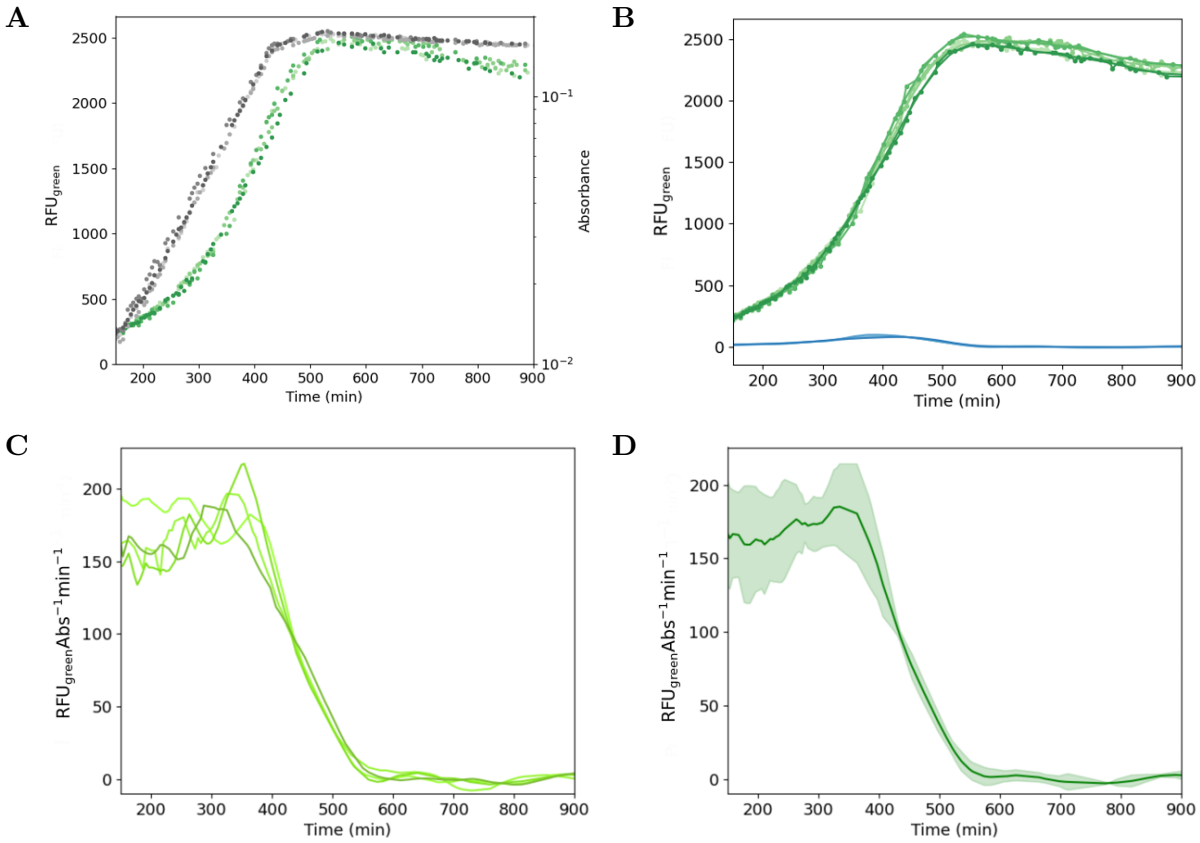

Figure S6: Reconstruction of promoter activities from GFP data of bacteria growing in minimal medium with xylose. (**A**) Green fluorescence (green dots) and absorbance (grey to black dots) for 4 replicates. (**B**) Estimation of $Im(t)$ (blue curves) and $M(t)$ (green curves) using the GFP maturation model and the data from panel A, also presented here (green dots). (**C**) Reconstruction of individual promoter activities for each replicate using the Bayesian inference procedure. (**D**) Mean of reconstructed promoter activities and confidence intervals given by two times the standard error of the mean. The curve in panel D corresponds to the promoter activity profile shown in Fig. 3E in the main text.

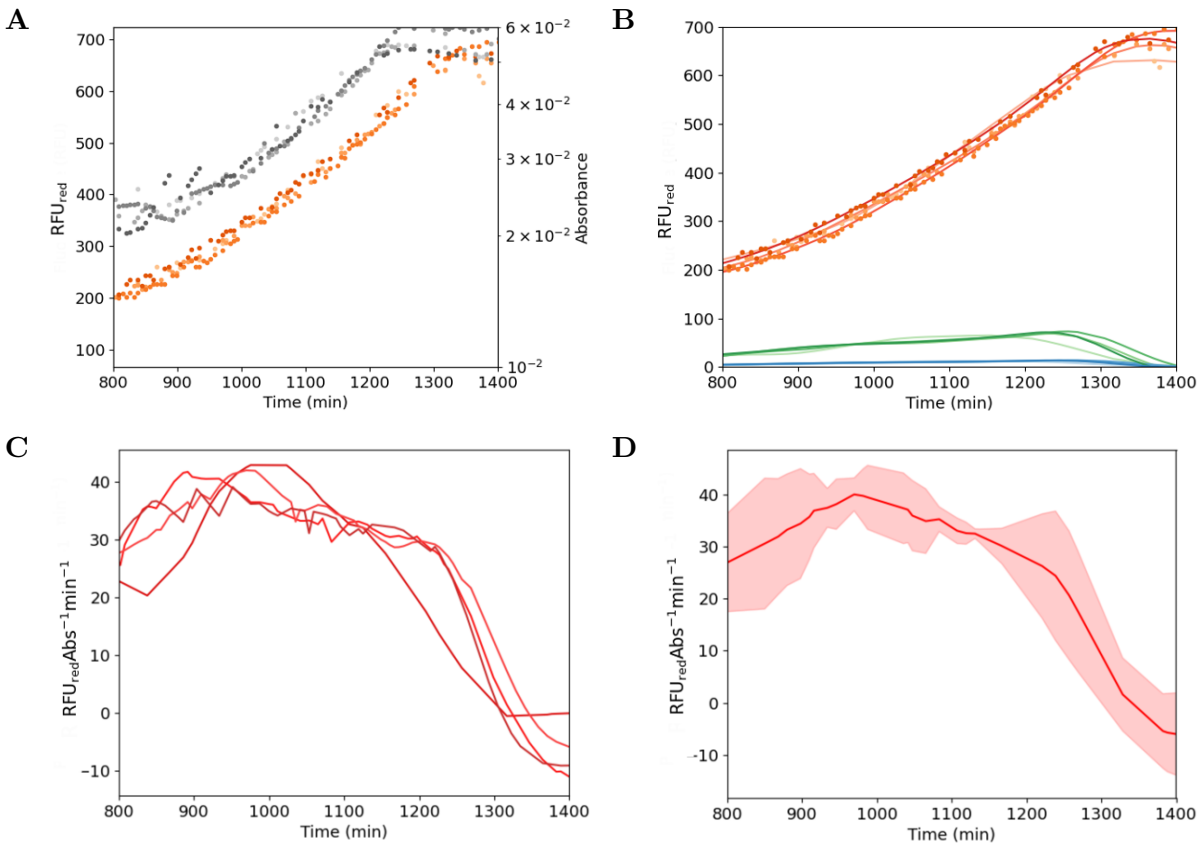

Figure S7: Reconstruction of promoter activities from RFP data of bacteria growing in minimal medium with acetate. (**A**) Red fluorescence (orange to red dots) and absorbance (grey to black dots) for 4 replicates. (**B**) Estimation of $Im(t)$ (green curves), $Hm(t)$ (blue curves) and $M(t)$ (orange to red curves) using the RFP maturation model and the data from panel A, also presented here (orange to red dots). (**C**) Reconstruction of individual promoter activities for each replicate using the Bayesian inference procedure. (**D**) Mean of reconstructed promoter activities and confidence intervals given by two times the standard error of the mean.

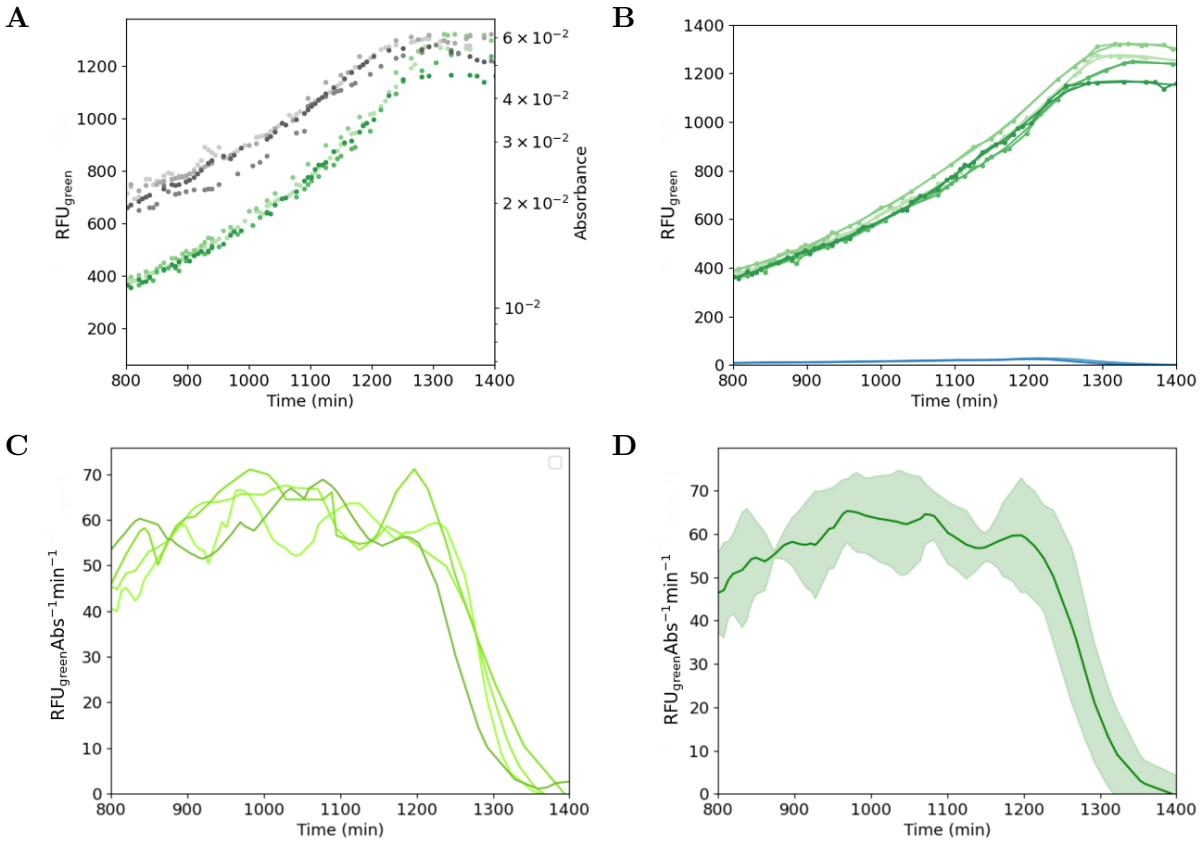

Figure S8: Reconstruction of promoter activities from GFP data of bacteria growing in minimal medium with acetate. (**A**) Green fluorescence (green dots) and absorbance (grey to black dots) for 4 replicates. (**B**) Estimation of $Im(t)$ (blue curves) and $M(t)$ (green curves) using the GFP maturation model and the data from panel A, also presented here (green dots). (**C**) Reconstruction of individual promoter activities for each replicate using the Bayesian inference procedure. (**D**) Mean of reconstructed promoter activities and confidence intervals given by two times the standard error of the mean.

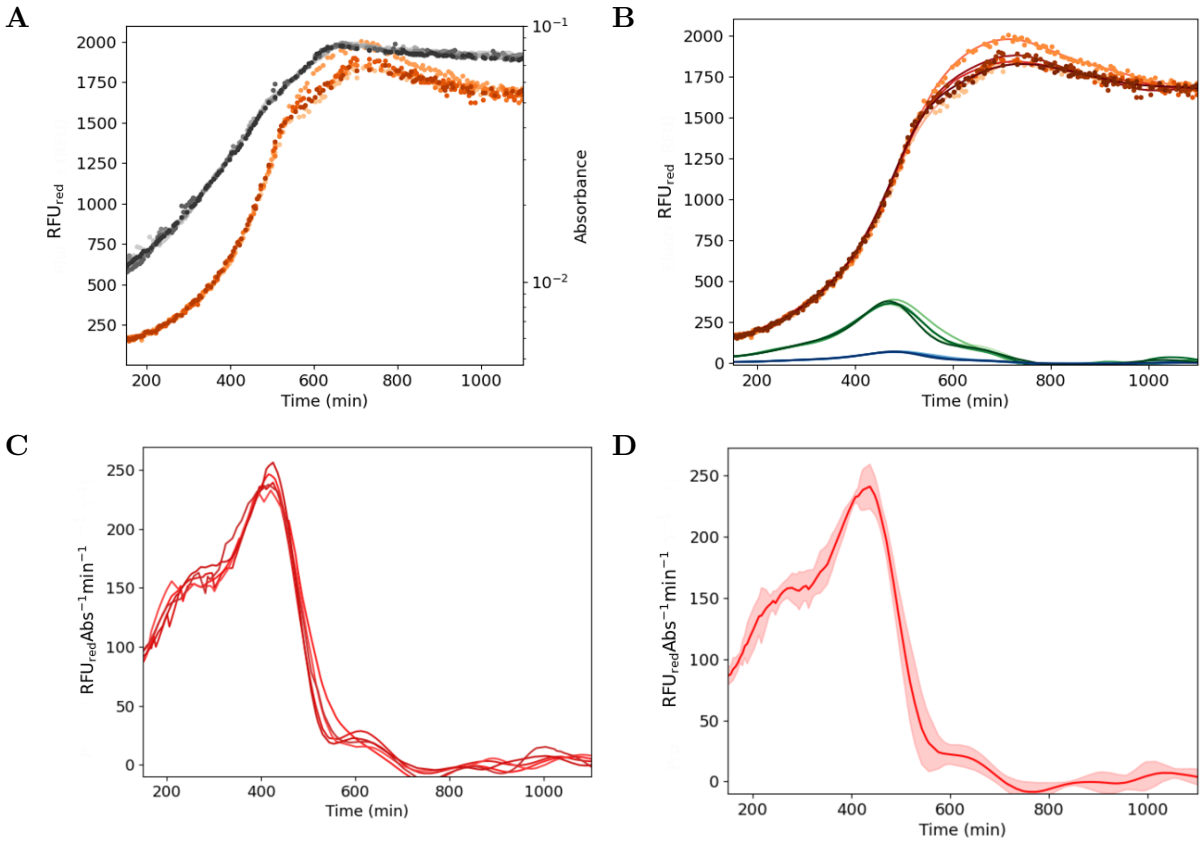

Figure S9: Reconstruction of promoter activities from RFP data of bacteria growing in minimal medium with pyruvate. (**A**) Red fluorescence (orange to red dots) and absorbance (grey to black dots) for 4 replicates. (**B**) Estimation of $Im(t)$ (green curves), $Hm(t)$ (blue curves) and $M(t)$ (orange to red curves) using the RFP maturation model and the data from panel A, also presented here (orange to red dots). (**C**) Reconstruction of individual promoter activities for each replicate using the Bayesian inference procedure. (**D**) Mean of reconstructed promoter activities and confidence intervals given by two times the standard error of the mean.

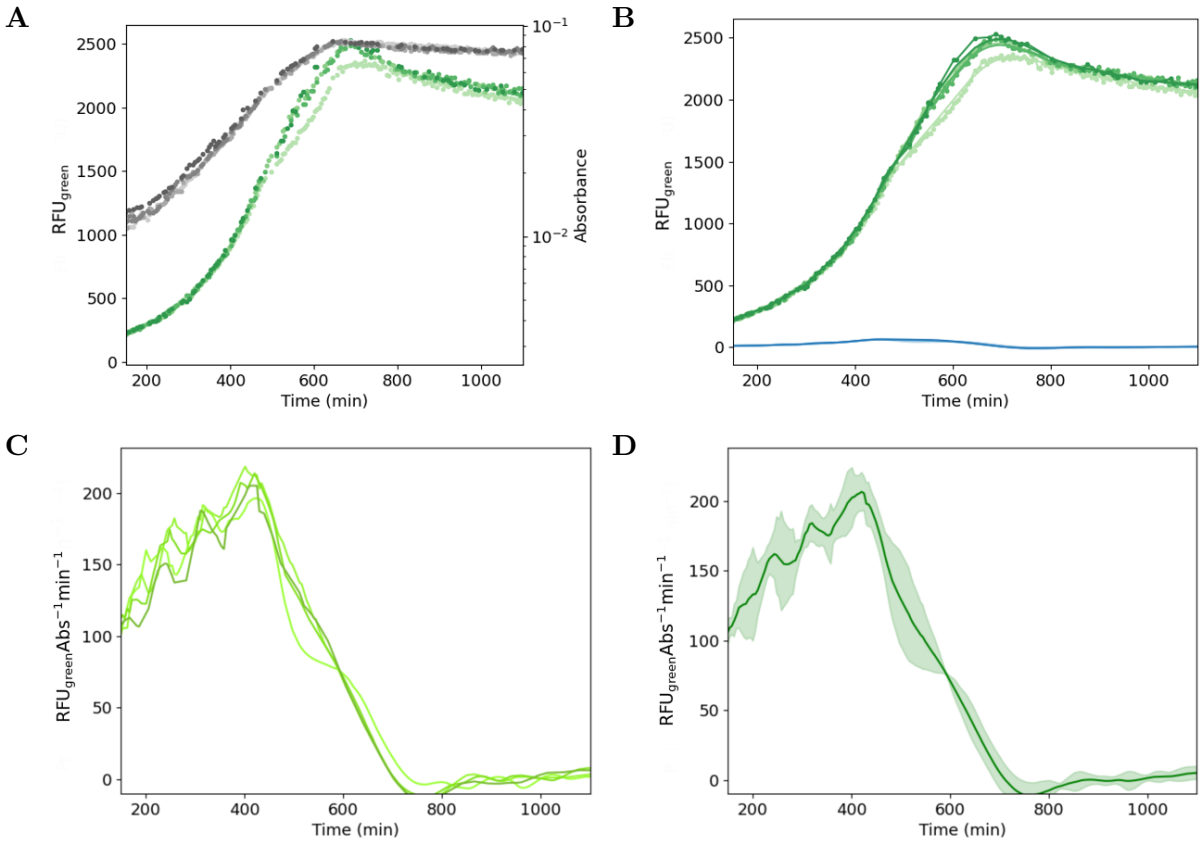

Figure S10: Reconstruction of promoter activities from GFP data of bacteria growing in minimal medium with pyruvate. (**A**) Green fluorescence (green dots) and absorbance (grey to black dots) for 4 replicates. (**B**) Estimation of $Im(t)$ (blue curves) and $M(t)$ (green curves) using the GFP maturation model and the data from panel A, also presented here (green dots). (**C**) Reconstruction of individual promoter activities for each replicate using the Bayesian inference procedure. (**D**) Mean of reconstructed promoter activities and confidence intervals given by two times the standard error of the mean.

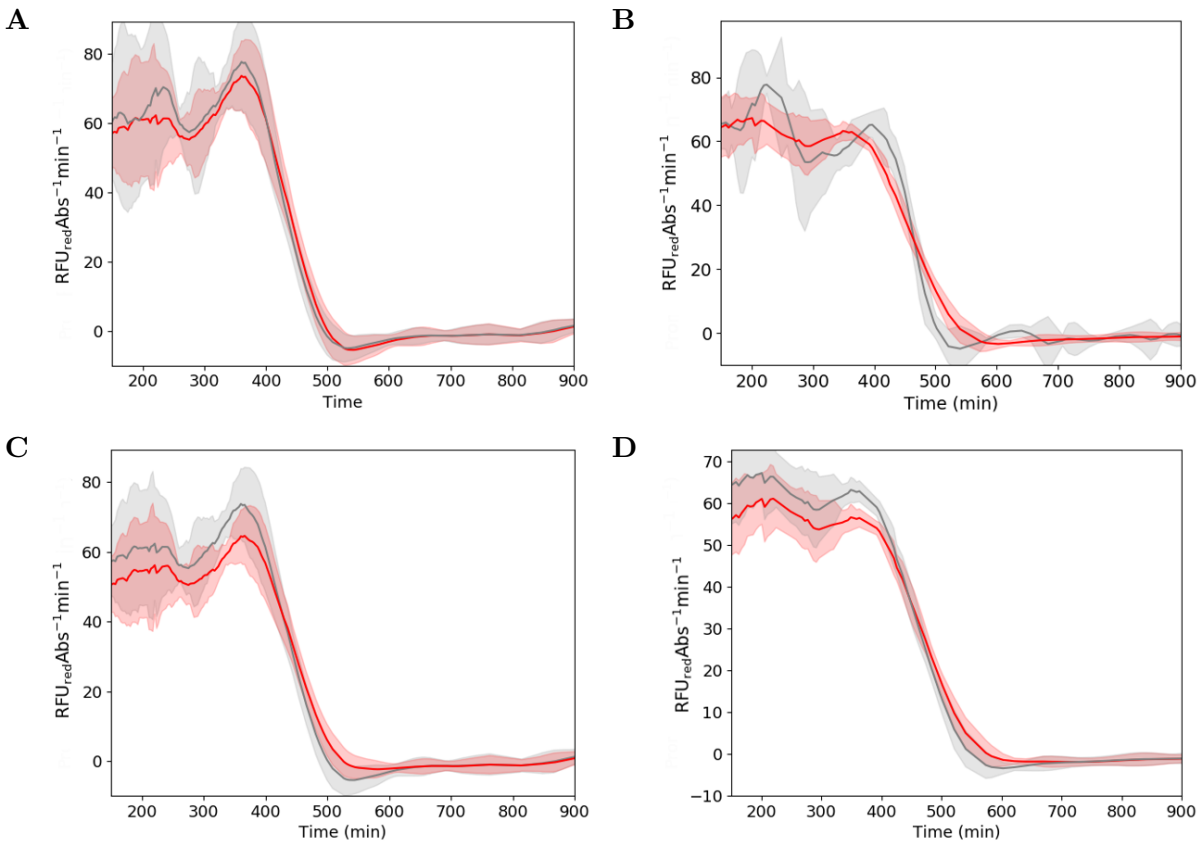

Figure S11: Reconstruction of promoter activities from RFP data using one-step models for maturation correction and/or published maturation times. (**A**) Promoter activities reconstructed from RFP data in the case of growth in minimal medium with glucose (Fig. 3B), using a one-step model fitted against red fluorescence data from the calibration experiment (Fig. 1C). The plot shows the mean over eight replicates (red curve) and a confidence interval given by twice the standard error of the mean. For reference, we also show the promoter activity obtained with the reference model (grey curve and confidence bands, reproduced from Fig. 3D). The mean promoter activities obtained from the two-step and the one-step models show a high correspondence ($R^2 = 0.99$). (**B**) Idem, but for growth in minimal medium with xylose, using data from Fig. 1D and Fig. 3C ($R^2 = 0.98$). (**C**) As in panel A, but when using the published maturation constant for mScarlet-I from Balleza *et al.* [1]. Again, there is a very good quantitative correspondence ($R^2 = 0.997$). (**D**) Idem, but for growth in minimal medium with xylose ($R^2 = 0.998$).

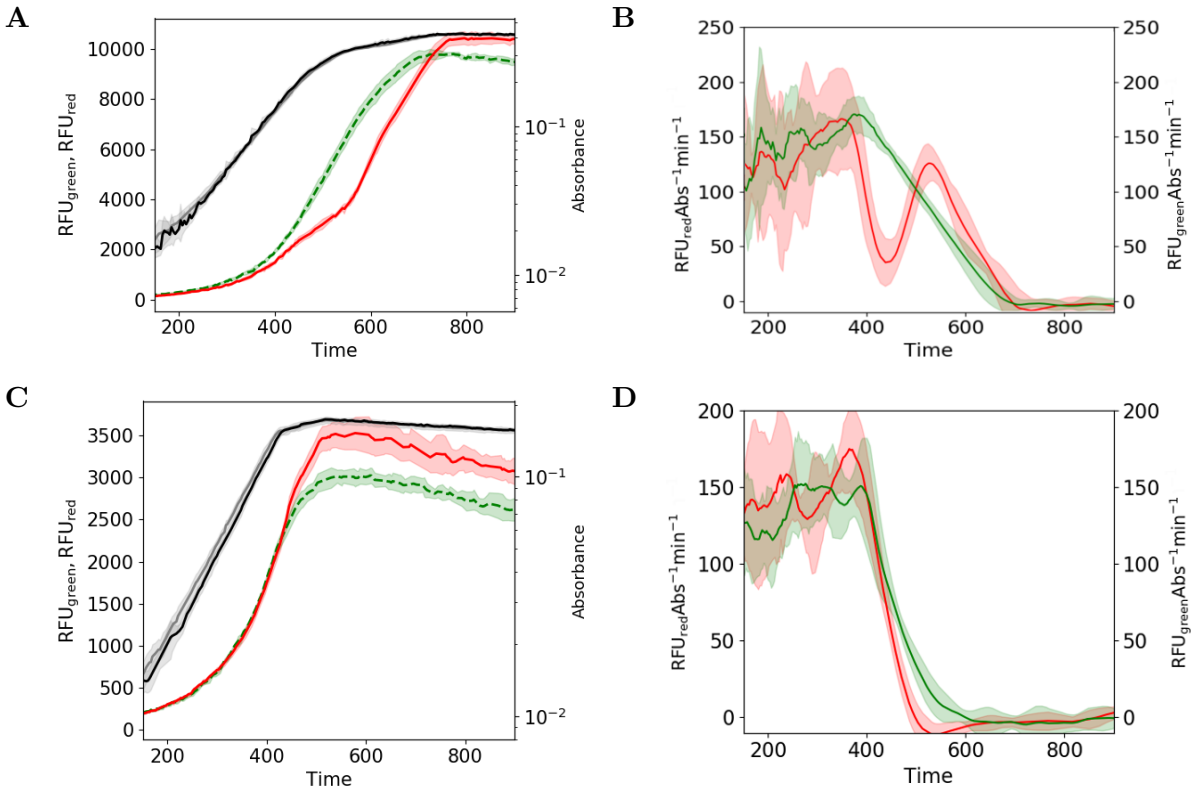

Figure S12: Reconstruction of promoter activities in bacterial cultures grown to high biomass densities. (**A**) Strains expressing RFP and GFP were grown in minimal medium supplemented with 0.2% glucose (black and grey curves for biomass, and red and green curves for fluorescence measurements, respectively). (**B**). Promoter activities reconstructed from the data in panel A, using the calibrated GFP and RFP maturation models of Eqs 1-5. The plot shows the mean over 8 replicates (red or green curve) and a confidence interval given by twice the standard error of the mean. A limitation of oxygen at high biomass densities most likely entails delays in the maturation of RFP and causes a dip in the promoter activity as explained in the *Discussion* of the main text.

A

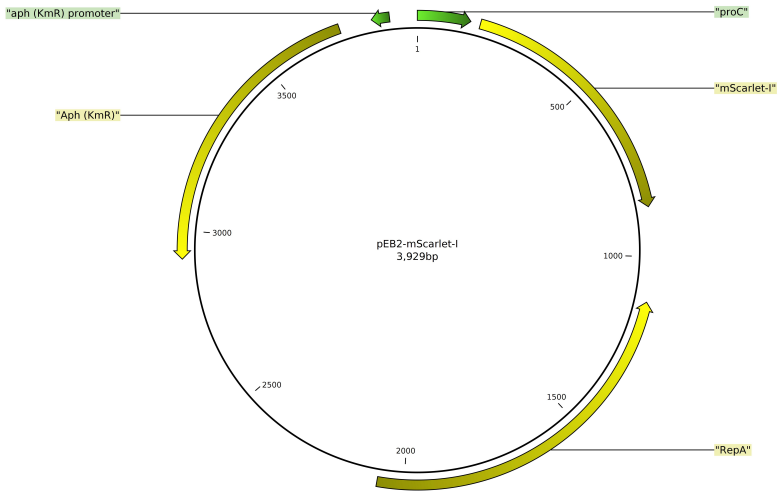

B

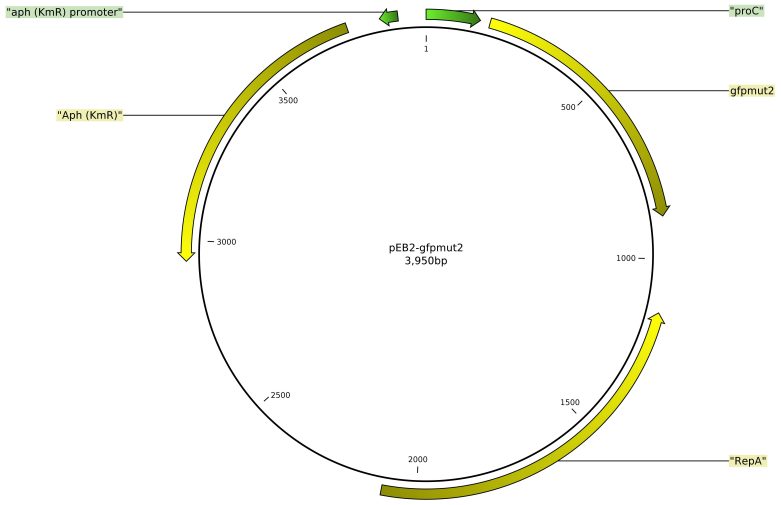

Figure S13: Plasmid design. (**A**) pEB2-mScarlet-I plasmid. (**B**) pEB2-gfpmut2 plasmid. Details on plasmid construction can be found in the *Materials and methods*. The plasmid sequences are available as File S2. We used the following primer sequences: gfpmut2_gib_pEb2_fw: GAACTATACAAATAAATGTCCAGACCTGCA, gfpmut2_gib_pEb2_rv: GAAGGAGATATACATATGAGTAAAGGAGAAGAACTTTTC, pEB2_gib_gfpmut2_fw: GAACTATACAAATAAATGTCCAGACCTGCAG and pEB2_gib_gfpmut2_rv: TTCTCCTTTACTCATATGTATATCTCCTTCTTAAATCTAGAAAAG

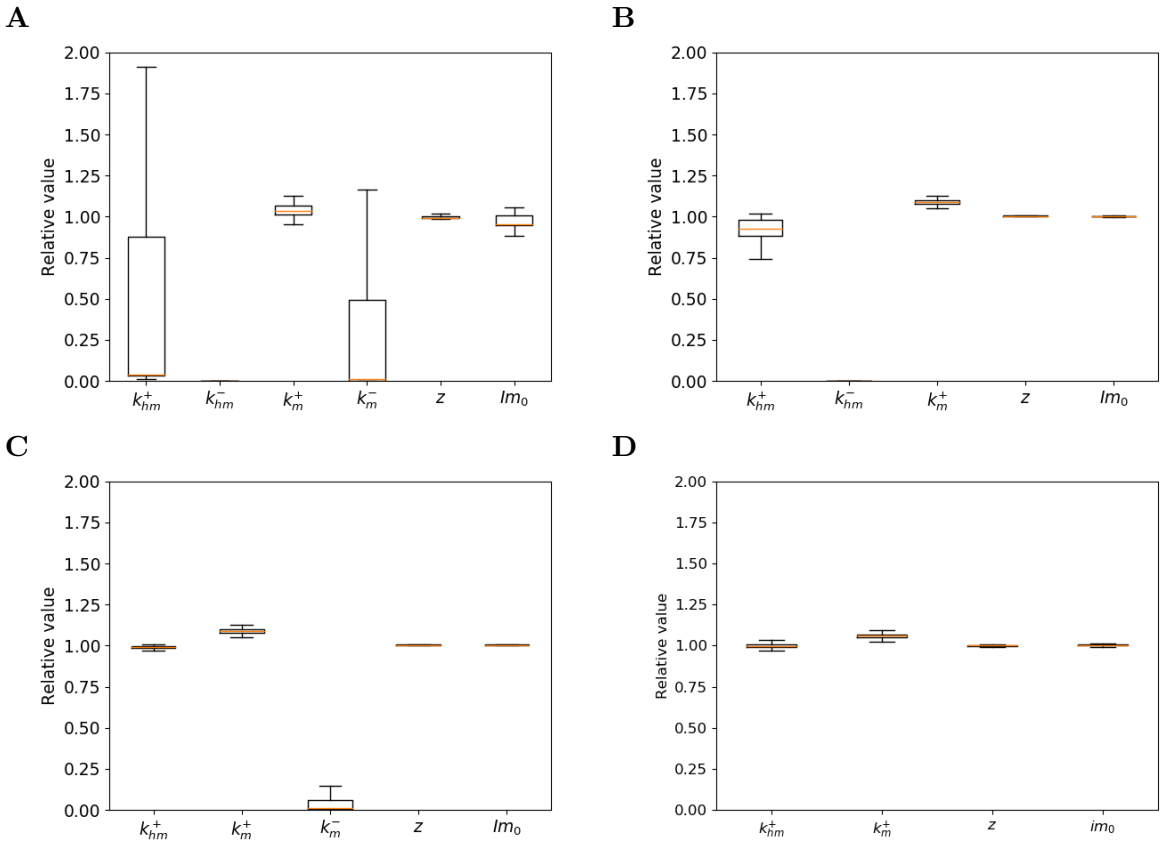

Figure S14: Results of identifiability analysis using a bootstrapping procedure. The four alternative RFP models were used alongside a bootstrapping procedure described to check the robustness of the estimation procedure and signal identifiability issues (*Materials and methods* and Text S1). The parameter value obtained from the actual dataset were divided by the ones returned by the bootstrapping procedure. The center of each box represents the median and its height the interquantile range. The whiskers represent the minimum and maximum of each estimate. Models I-IV: panels **A-D**, respectively. The parameter values in Model IV are precisely determined, whereas the other models have identifiability issues.

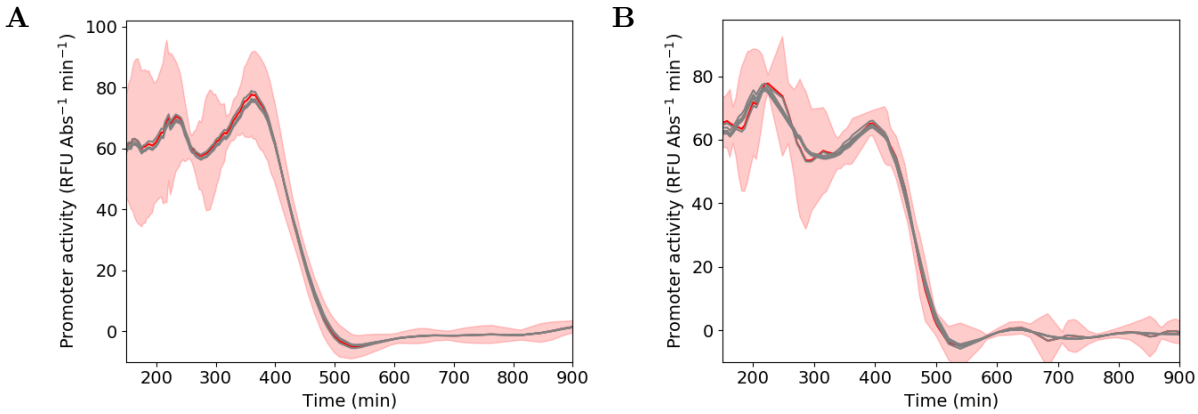

Figure S15: Effect of varying parameter values on the reconstruction of promoter activities. (**A**) Promoter activity (mean and confidence interval, red curve and band) reconstructed from the RFP data in the case of growth in minimal medium with glucose (Fig. 3D). We repeated the analysis using the same model, but with parameter values from within the interquantile range in Fig. S14D. Ten sample promoter activities for alternative parameter values (grey curves) are shown and seen to fall within the confidence interval of the original estimate. (**B**) Idem, but for growth in minimal medium with xylose, as compared to the reference from Fig. 3E.

References

[1] Balleza, E., J. M. Kim, and P. Cluzel, 2018. Systematic characterization of maturation time of fluorescent proteins in living cells. *Nat Methods* 15:47–51.